

1 **Headwater stream length dynamics across four physiographic provinces of the**
2 **Appalachian Highlands**

3
4 Carrie K. Jensen^{a,b*}, Kevin J. McGuire^{a,b}, and Philip S. Prince^c

5 ^a Department of Forest Resources and Environmental Conservation (MC 0324), Cheatham Hall
6 RM 313, Virginia Tech, 310 West Campus Drive, Blacksburg, VA 24061, USA, E-mail:
7 ckjensen@vt.edu, Telephone: +1 (540) 231-6017

8 ^b Virginia Water Resources Research Center (MC 0444), Cheatham Hall STE 210, Virginia
9 Tech, 310 West Campus Drive, Blacksburg, VA 24061, USA, E-mail: kevin.mcguire@vt.edu

10 ^c Department of Geosciences (MC 0420), Derring Hall RM 4044, Virginia Tech, 926 West
11 Campus Drive, Blacksburg, VA 24061, USA, E-mail: psprince@vt.edu

12
13 * Corresponding author

14
15 This is the peer reviewed version of the following article: Jensen CK, McGuire KJ, Prince
16 PS. Headwater stream length dynamics across four physiographic provinces of the Appalachian
17 Highlands. *Hydrological Processes*. 2017;31:3350–3363, which has been published in final form
18 at <https://doi.org/10.1002/hyp.11259>. This article may be used for non-commercial purposes in
19 accordance with Wiley Terms and Conditions for Self-Archiving.

24 **Abstract**

25 Understanding patterns of expansion, contraction, and disconnection of headwater stream
26 length in diverse settings is invaluable for the effective management of water resources as well
27 as for informing research in the hydrology, ecology, and biogeochemistry of temporary streams.
28 More accurate mapping of the stream network and quantitative measures of flow duration in the
29 vast headwater regions facilitate implementation of water quality regulation and other policies to
30 protect waterways. We determined the length and connectivity of the wet stream and geomorphic
31 channel network in three forested catchments (<75 ha) in each of four physiographic provinces
32 of the Appalachian Highlands: the New England, Appalachian Plateau, Valley and Ridge, and
33 Blue Ridge. We mapped wet stream length seven times at each catchment to characterize flow
34 conditions between exceedance probabilities of <5% and >90% of the mean daily discharge.
35 Stream network dynamics reflected geologic controls at both regional and local scales. Wet
36 stream length was most variable at two Valley and Ridge catchments on a shale scarp slope and
37 changed the least in the Blue Ridge. The density and source area of flow origins differed
38 between the crystalline and sedimentary physiographic provinces, as the Appalachian Plateau
39 and Valley and Ridge had fewer origins with much larger contributing areas than New England
40 and the Blue Ridge. However, the length and surface connectivity of the wet stream depended on
41 local lithology, geologic structure, and the distribution of surficial deposits such as boulders,
42 glacially-derived material, and colluvial debris or sediment valley fills. Several proxies indicate
43 the magnitude of stream length dynamics, including bankfull channel width, network
44 connectivity, the base flow index, and the ratio of geomorphic channel to wet stream length.
45 Consideration of geologic characteristics at multiple spatial scales is imperative for future
46 investigations of flow intermittency in headwaters.

47

48 **Keywords:** temporary streams; drainage density; headwaters; physiographic provinces; stream
49 length; flow intermittency; geomorphic channel; Appalachian Highlands

50

51

52 **1. Introduction**

53 Nearly half of first- and second-order headwaters consist of temporary ephemeral and
54 intermittent streams that expand and contract seasonally or in response to storm events (Nadeau
55 and Rains, 2007; Buttle et al., 2012; Datry et al., 2014). Headwaters provide essential ecosystem
56 services, including flood attenuation, biogeochemical cycling, and aquatic habitat (Larned et al.,
57 2010) yet are challenging to characterize and study due to their dynamic nature, enormous
58 extent, and remote or inaccessible locations. As a result, maps of the stream network are often
59 inaccurate (Bishop et al., 2008; Skoulikidis et al., 2017). Common representations of river
60 networks such as the National Hydrography Dataset (NHD) in the U.S. underestimate headwater
61 length by up to 200% (Fritz et al., 2013) and fail to indicate the range of drainage density values
62 that can easily span an order of magnitude (Gregory and Walling, 1968). The basic task of
63 locating where and when streams are flowing has myriad implications for watershed policy and
64 management activities like the delineation of riparian buffers and implementation of best
65 management practices (BMPs). Quantitative data on the frequency and duration of flow in
66 temporary streams across broad geographic regions would enable more targeted conservation
67 efforts to ensure the ecological integrity of headwaters as well as downstream waterways.

68 Variability in headwater length produces a suite of landscape functions that shift through
69 time. Channelized surface flow efficiently transports water, sediment, and solutes to water

70 supplies destined for human consumption (Alexander et al., 2007) when stream length and
71 connectivity are high. Accordingly, BMPs are more stringent for streams designated as perennial
72 on maps (Blinn and Kilgore, 2001; National Research Council, 2002). Headwater networks often
73 become discontinuous during low flows, with wet reaches separated by intervening dry channel
74 segments (Stanley et al., 1997). Surface water-ground water exchange occurs between
75 disconnected reaches via hyporheic flow paths that moderate water temperatures, provide habitat
76 refugia, and facilitate biogeochemical reactions such as denitrification (Boulton et al., 1998).
77 Alternating patches of flowing water, dry channel bed, and standing pools simultaneously
78 transport, store, and process organic matter, nutrients, and toxins, creating opportunities for both
79 aerobic and anaerobic transformations (Larned et al., 2010). In addition, Cohen et al. (2016)
80 emphasize the ecological benefits that result from a *lack* of surface or subsurface connection
81 between water bodies. Dry channels serve as egg and seed banks for aquatic species and
82 retention sites to slow the downstream movement of sediment, organic matter, and contaminants
83 (Steward et al., 2012). Thus, metrics describing not only stream length but the connectivity and
84 configuration of wet and dry reaches are necessary to accurately model available habitat and
85 species distributions, pollutant transmission, and rates of biogeochemical processes.

86 Early hydrological investigations recognized that headwater stream length is not static
87 (Hewlett and Hibbert, 1967; Gregory and Walling, 1968; Morgan, 1972; Roberts and Klingeman,
88 1972; Blyth and Rodda, 1973; Day, 1978; Day, 1980), but, as Godsey and Kirchner (2014)
89 highlight, the topic was largely abandoned until the early 2000s, with some notable exceptions
90 (Calver, 1990; De Vries, 1994). Following growing recognition of the legal considerations of
91 headwaters and their significance for aquatic ecosystems (Doyle and Bernhardt, 2010; Acuña et
92 al., 2014), interest in the expansion and contraction of temporary networks has renewed in recent

93 years. However, measuring changes in stream length is challenging (Wharton, 1994). Several
94 mapping studies involve walking the entire stream network of watersheds multiple times
95 (Godsey and Kirchner, 2014; Shaw, 2016, Whiting and Godsey, 2016; Zimmer and McGlynn,
96 2017). Owing to the time and effort required to traverse rough terrain, field campaigns are
97 usually limited to mapping a few catchments in the same region seasonally—e.g., 4 catchments
98 over 3 or 4 mapping dates (Godsey and Kirchner, 2014; Whiting and Godsey, 2016)—or a single
99 watershed more frequently—e.g., 12 (Shaw, 2016) or 77 mapping surveys (Zimmer and
100 McGlynn, 2017). At a coarser scale, other studies locate intermittent and perennial flow origins
101 during wet and dry seasons, respectively, without noting disconnections in the stream network or
102 the position of origins during intermediate flows or after storms (Paybins, 2003; Jaeger et al.,
103 2007; Russell et al., 2015; Brooks and Colburn, 2011). Electrical resistance sensors that detect
104 the presence or absence of water are increasingly popular for monitoring channel wetting and
105 drying at a fine temporal resolution (Jaeger and Olden, 2012; Goulsbra et al., 2014; Peirce and
106 Lindsay, 2015). These sensors determine the timing of flow more accurately and require less data
107 interpretation than temperature-based methods (Blasch et al., 2002). Although electrical
108 resistance sensors are one of the cheapest ways to automatically detect stream flow, the cost of
109 \$75-100 per sensor (Blasch et al., 2002; Chapin et al., 2014) renders dense instrumentation of
110 large or multiple networks impractical. Aerial photographs (Wigington et al., 2005) and
111 unmanned aerial vehicles can also aid temporary stream mapping, but image processing is labor-
112 intensive, and clear views of the stream are not always possible in densely vegetated areas
113 (Spence and Mengistu, 2016).

114 While temporary stream research continues to advance, headwater networks vary across
115 the tremendous diversity of landscapes in the world, reflecting complex combinations of

116 climatic, geologic, ecological, and land use factors (Costigan et al., 2016).). This inherent
117 complexity precludes the generalization of a single, straightforward rule that encapsulates all
118 headwater behavior (Bishop et al., 2008). Owing to the logistical difficulties of examining
119 headwater processes over large areas, studies are almost always site-specific and conducted at
120 the scale of small watersheds or even hillslopes. Although the detail possible at these finer scales
121 is necessary to adequately characterize headwaters, we must extend our focus to understand
122 regional trends that may be more applicable to managing water resources.

123 Costigan et al. (2016) recognize geology as one of the three major controls on flow
124 permanence, in addition to climate and land cover. Studies demonstrate that the underlying
125 geology correlates to the mobility of flow origins (Paybins, 2003; Jaeger et al., 2007; Winter,
126 2007) and variability of stream length (Day, 1980; Whiting and Godsey, 2016). Geology also
127 impacts geomorphic channel development and the resulting drainage density (Hadley and
128 Schumm, 1961; Abrahams, 1984). The purpose of this project is to further investigate the role of
129 geology in headwater stream length dynamics along a physiographic gradient in the Appalachian
130 Highlands. We mapped three catchments in each of four physiographic provinces seven times
131 across multiple flow conditions. Research questions include: (1) How do stream length, network
132 connectivity, and the number and upslope area of flow origins change with runoff and the
133 associated exceedance probability? (2) At what flow does the wet stream approximate
134 geomorphic channel length? (3) Do stream length dynamics vary systematically by
135 physiographic province?

136

137 **2. Study Areas**

138 We examined forested headwater catchments from study areas spanning four
139 physiographic provinces of the Appalachian Highlands: the Hubbard Brook Experimental Forest
140 (HB) of New Hampshire in New England, Fernow Experimental Forest (FNW) in the
141 Appalachian Plateau of West Virginia, Jefferson National Forest at Poverty Creek (PVY) and the
142 South Fork of Potts Creek (SFP) in the Valley and Ridge of Virginia, and the Coweeta
143 Hydrologic Laboratory (CWT) in the Blue Ridge of North Carolina (Figure 1). HB, FNW, and
144 CWT are experimental watersheds overseen by the U.S. Forest Service and, thus, have gauged
145 catchments, long-term hydroclimatic datasets, and reference areas that do not undergo
146 experimental manipulation. We chose PVY and SFP because of their location on National
147 Forest, full coverage by mature forest, relatively easy access by road, and the availability of a 3
148 m Digital Elevation Model (DEM).

149 The study areas exhibit a range of climate (Table 1), geology (Table 2), topography
150 (Table 2), and vegetation. HB is located in the central highlands of New England in the White
151 Mountain National Forest. HB is the coldest site, and stream flow peaks in the late spring
152 following snowmelt. Rounded, hummocky topography is typical of the glacial HB landscape.
153 The study catchments are underlain by Lower Silurian pelitic schist and calc-silicate granulite of
154 the Upper and Lower Rangeley Formation (Barton, 1997) and have a mantle of basal and
155 ablation till and reworked glacial drift derived from Early Devonian granodiorite of the Kinsman
156 Formation and other granitic, metasedimentary, and metavolcanic units (Bailey, S. et al., 2003).

157 FNW lies within the Allegheny Mountains of the Appalachian Plateau in the
158 Monongahela National Forest. The greatest rainfall generally occurs from May to July in the
159 form of high-intensity convective thunderstorms. The Alleghenies have a gently folded structure
160 characterized by low-amplitude folds with strata displaying low ($<10^\circ$) and often nearly

161 horizontal dip. Partial dissection of the landscape has produced steep slopes leading to broad, flat
162 uplands. Devonian shales and sandstones of the Hampshire Formation form the bedrock at FNW
163 (Cardwell et al., 1968).

164 PVY and SFP are part of the Jefferson National Forest in Montgomery and Giles
165 Counties, Virginia. The catchments lie in a rain shadow in the central Valley and Ridge,
166 receiving the least precipitation of the study areas. Precipitation is usually highest from May to
167 July, but stream flows peak during the winter and early spring. Erodibility contrasts within
168 strongly folded and thrust faulted sedimentary rock in the Valley and Ridge create parallel ridges
169 and distinct trellis drainage patterns. Bedrock at PVY is made up of Devonian shales, siltstones,
170 and sandstones of the Brallier and Chemung Formations (Virginia Division of Mineral
171 Resources, 1993). SFP is underlain by Devonian Oriskany sandstones at lower elevations and by
172 Silurian Keefer and Rose Hill sandstones at higher elevations (Schultz et al., 1986).

173 CWT is located in the Nantahala National Forest in the Southern Blue Ridge Mountains.
174 CWT is both the warmest and wettest of the study areas. Precipitation is greatest in the winter
175 and early spring and increases with elevation (Laseter et al., 2012). Intensely deformed
176 metamorphic rock is exposed in an extremely steep, rugged, and relatively high-elevation
177 landscape. The substrate consists of Middle to Late Proterozoic biotite gneiss and amphibolite of
178 the Coweeta Group and Tallulah Falls Formation (Hatcher, 1988) that has weathered into thick
179 saprolite (on average 6 m; Price et al. 2005) due to the warm, humid climate.

180 Logging occurred at all sites through the early twentieth century. Second-growth forests
181 range from primarily northern hardwoods at HB to oak-hickory associations at CWT. Unlike the
182 other study areas, PVY and SFP are not part of an experimental forest and have been subject to

183 more recent timber harvests. Forests at PVY and SFP are mature (~60 years old) but are
184 estimated to be a few decades younger than at HB, FNW, and CWT.

185

186 **3. Methods**

187 *3.1 Site selection*

188 We selected three catchments smaller than 45 ha with no recent history of logging or
189 experimental treatment in each study area (Table 2). SFP70 is the only exception at 70 ha. We
190 determined during field work at HB and CWT that a 40-45 ha catchment requires a full day to
191 map the stream network. Mapping larger watersheds over multiple days increases the risk of
192 precipitation events in the humid Appalachians and widens the range of discharge pertaining to
193 the mapped wet stream length. Perennial stream flow in the Appalachians frequently begins at
194 smaller catchment source areas than in arid regions (Rivenbark and Jackson, 2004), so mapping
195 downstream of persistent flow may not be necessary to address the question of stream length
196 variability. However, many Valley and Ridge headwaters contract to a few isolated pools and
197 flowing reaches during the late summer. We ultimately decided to include two Valley and Ridge
198 catchments within the given size constraints (PVY25 and PVY35) and another larger site with a
199 greater length of perennial flow (SFP70) to be consistent with the other study areas that all have
200 perennial streams at the catchment outlets. For this study, we adhere to the definition of
201 perennial channels by Hedman and Osterkamp (1982) as having flow present more than 80% of
202 the year. Mapping of SFP70 was still possible within a day.

203 *3.2 Field mapping of the stream network*

204 We mapped the wet stream network of each catchment seven times at varying discharges.
205 We follow the general terminology of Day (1980) and Goulsbra et al. (2014) by referring to the

206 “wet” stream, but other studies use “flowing stream” (Calver, 1990; Godsey and Kirchner,
207 2014), “active channel network” (Shaw, 2016), “active drainage network” (Godsey and
208 Kirchner, 2014; Peirce and Lindsay, 2015; Whiting and Godsey, 2016), and “active surface
209 drainage length” (Zimmer and McGlynn, 2017). We did not want to use the term “flowing,” as
210 disconnected pools are not always visibly flowing downstream. Referring to surface water as
211 “active” can imply that hyporheic exchange and ground water flow in the subsurface are inactive
212 processes, unless specified as “active surface” water (Zimmer and McGlynn, 2017). We chose
213 “wet stream” because the term is simple, encompasses both flowing reaches and standing pools,
214 and avoids the term “channel,” which corresponds to a geomorphic feature. However, we
215 emphasize that “wet stream” only applies to surface water greater than 1 m in length and not to
216 damp or saturated channel sediments.

217 We walked along the stream during each mapping from the outlet until we located the
218 flow origin of every tributary. We continued walking upslope past the flow origins to make sure
219 the origins were points of surface flow initiation rather than a network disconnection. Flow
220 origins and disconnections were marked with a Bad Elf GNSS Surveyor Global Positioning
221 System (GPS) unit. We also mapped the geomorphic channel at each site as reaches with defined
222 banks (Dunne and Leopold, 1978) and sorted bed materials (Dietrich and Dunne, 1993)
223 regardless of surface flow. The GPS unit has 1 m reported accuracy, but accuracy was normally
224 between 3 and 10 m depending on vegetation cover and weather. Owing to the lower than
225 reported accuracy, we used field notes and pin flags marking the wet stream in addition to the
226 GPS points to compare stream length between mappings. The same individual performed all
227 mappings with the same GPS unit to ensure the maximum consistency possible. We measured
228 bankfull width and depth at 4 to 6 designated cross-sections distributed among the tributaries that

229 had a simple channel pattern and were clear of woody debris. We recorded water width and
230 depth at the cross-sections during each mapping as an indicator of the flow condition, since real-
231 time stream discharge data were not always available. Field work was completed at HB in the
232 summer of 2015, at FNW in the summer, fall, and winter of 2016, and at CWT and PVY/SFP in
233 the fall of 2015 and winter, spring, and summer of 2016.

234

235

236 *3.3 Stream discharge*

237 Eight of the twelve study sites are gauged with weirs measuring stream flow at 5-minute
238 intervals (sites that also have watershed numbers in Table 2). We developed flow duration curves
239 for each of the gauged catchments using 10 years (2006-2015) of mean daily flow data. We
240 determined discharge at the remaining catchments (HB25, PVY25, PVY35, and SFP70) during
241 each field visit using salt dilution gauging (Calkins and Dunne, 1970). Pressure transducers
242 installed at PVY25, PVY35, and SFP70 recorded stream stage every 30 minutes for six months
243 to create a stage-discharge curve and provide a continuous estimate of flow. We did not measure
244 stage at HB25 because the site is adjacent to long-term gauged catchments (WS7 and WS8) of a
245 similar size to permit an estimate of flow exceedance probabilities. We extended the six months
246 of discharge data at PVY/SFP to 10 years (2006-2015) of mean daily flow values based on U.S.
247 Geological Survey (USGS) gauges at John's Creek (02017500), Walker Creek (03173000), Wolf
248 Creek (03175500), and the South Fork of the Roanoke (02053800) with the Streamflow Record
249 Extension Facilitator (SREF version 1.0) software package from the USGS (Granato, 2009) to
250 develop flow duration curves for the three Valley and Ridge catchments.

251 We strove to map the streams at flows between at least the 25 and 75% exceedance
252 probabilities rather than major storms and droughts, as such extreme events are difficult to
253 capture during a single field season.. Hydrograph rises in response to storms occur rapidly in
254 mountain streams and depend on antecedent moisture and the amount and duration of
255 precipitation, which are hard to predict in advance. For this reason, we only mapped on the
256 recession limb of events at least several hours after the hydrograph peak and compared discharge
257 at the beginning and end of mapping to constrain the precision of our runoff (discharge
258 normalized by catchment area) calculations. We consulted nearby USGS gauges for approximate
259 flow conditions if real-time data for the study sites were not available.

260 *3.4 Network delineation*

261 We imported the GPS points into ArcGIS (ArcMap version 10.3.1, ESRI 2015, Redlands,
262 CA) and digitized the stream network along lines of high flow accumulation according to the
263 multiple triangular flow direction algorithm (Seibert and McGlynn, 2007) applied to 3 m DEMs
264 for all sites. All DEM processing was completed in ArcGIS and the System for Automated
265 Geoscientific Analyses software (SAGA version 2.3.1). The 1/9 arc-second DEMs for FNW,
266 CWT, and SFP are from the West Virginia and North Carolina National Elevation Dataset of
267 2003. LiDAR data were collected during leaf-off and snow-free conditions at PVY in 2011 for
268 the Virginia Geographic Information Network and at HB in 2012 by for the White Mountain
269 National Forest. Bare earth DEMs classified from the LiDAR datasets were re-sampled to 1 m
270 and coarsened to 3 m via mean cell aggregation. We applied a low-pass (3 x 3) filter and sink-
271 filling algorithm (Wang and Liu, 2006) to all DEMs for hydrological correction. We manually
272 moved points located in low flow accumulation pixels due to GPS error to the nearest cell of
273 high flow accumulation. We did not move points more than 3 pixels (9 m) based on the average

274 GPS accuracy. Field notes aided this process to verify that point displacements were due to a
275 change in stream length instead of positional error. Overall, we found the flow accumulation grid
276 to be quite consistent with the GPS point locations.

277 We calculated several metrics from the digitized stream networks. We found wet
278 drainage density by dividing the total length of wet reaches by the catchment area. Drainage
279 density was similarly found for the geomorphic channel. Maximum network extent refers to the
280 entire stream length from the outlet to flow origins, including intervening dry reaches. When
281 considering subsurface flow between disconnected reaches, maximum network extent provides a
282 more comprehensive stream length estimate. Network connectivity equals the total wet stream
283 length divided by the maximum network (wet and dry) extent, and flow origin density is the
284 number of origins normalized by catchment area. We also found the upslope area (Seibert and
285 McGlynn, 2007) for each flow origin and geomorphic channel head. Following the method of
286 Godsey and Kirchner (2014), we calculated the slope of the power-law relationship (β) between
287 wet stream length and runoff for each site. We also determined Pearson product-moment
288 correlation coefficients between β values and our wet stream and geomorphic channel metrics in
289 addition to the base flow index (Lyne and Hollick, 1979) derived for each catchment.

290

291 **4. Results**

292 *4.1 Wet stream pattern and metrics*

293 We mapped the catchments across flows spanning exceedance probabilities of 3 and 90%
294 at HB, 6 and 93% at FNW, 3 and 92% at PVY, 2 and 95% at SFP, and 0.1 and 99% at CWT
295 (Figure 2). The pattern and flow duration of stream networks display contrasts between sites
296 from both a planform (Figure 3) and longitudinal perspective (Figure 4). Animations of network

297 contraction with decreasing runoff are available in the online supplementary material (Figures
298 S1-S12). The HB catchments produced numerous closely spaced tributaries in the plan view
299 (Figure 3), whereas the network pattern was quite simple at FNW. Watersheds at CWT had one
300 or two main channel stems but many bedrock springs that contributed short reaches along
301 tributaries, which was most evident at CWT33. SFP70 developed short, isolated reaches at both
302 high and low flows that did not form a surface connection with the rest of the network during any
303 mappings. We observed that three of these high flow duration reaches were actually small
304 wetlands at topographic lows with no inlet or outlet. The remaining reaches occurred on talus
305 slopes or boulder-filled hollows. We heard water flowing under the boulders during the two
306 wettest mappings; in these cases, water only emerged on top of the coarse deposits for short
307 distances, possibly upon encountering a less conductive sediment lens. Coarse surficial material
308 also coincided with the short, disconnected tributaries in the southeastern portion of HB42. Some
309 of the larger stream disconnections at FNW37, CWT12, and CWT40 were associated with old
310 landslide deposits where sediment depth locally increases. We observed that wetting and drying
311 patterns at PVY and SFP frequently reflected the degree of valley confinement; reaches with
312 steep valley side slopes and exposed bedrock had longer flow duration than unconfined sections
313 with a wide, sediment-filled valley floor.

314 Stream longitudinal profiles suggest that higher-elevation tributaries that have not yet
315 incised to the level of the main stem tended to dry up first, as was most evident for HB42,
316 PVY25, PVY35, and CWT12 (Figure 4). In the case of HB42, the reaches with relatively low
317 flow duration at shorter distances upstream were the southeastern disconnected tributaries in
318 boulder deposits, which prevent channel downcutting (Figure 3). The streams at HB13 and HB25

319 all interestingly occurred at a similar elevation for a given distance upstream, perhaps
320 corresponding to a water availability threshold or incision depth related to elevation.

321 Flow duration was greatest and most consistent at CWT and FNW14 and was lowest as
322 well as more spatially variable at PVY (Figures 3 and 4). Wet drainage density (km/km²) at each
323 study area ranged across mapping periods from 1.8 to 11 at HB, 0.5 to 3.0 at FNW, 0.1 to 6.1 at
324 PVY, 0.9 to 2.0 at SFP, and 3.2 to 6.1 at CWT. HB tended to have the highest wet stream length
325 for a given runoff (Figure 5) and associated exceedance probability (Figure 2). CWT sites
326 maintained moderate-high stream lengths that changed little with discharge. FNW and PVY
327 typically had shorter networks than HB and CWT for low flows with high exceedance
328 probabilities, but more similar lengths at higher runoffs. Stream length at SFP did not decrease
329 drastically at low runoffs like the other Valley and Ridge catchments at PVY, but rather followed
330 a trajectory similar to FNW and HB.

331 The number and mean upslope area of flow origins differed markedly between
332 physiographic provinces (Figure 5). FNW, PVY, and SFP in the Appalachian Plateau and Valley
333 and Ridge had fewer flow origins with greater upslope areas than HB and CWT. Across all sites
334 and mappings, HB in New England had the highest and most variable number of origins (Figure
335 6). Mean upslope area decreased slightly overall as runoff increased (Figure 5). Average upslope
336 area was smallest at HB, but was also low for CWT. The number of flow origins remained
337 practically the same for most mappings. One exception was SFP70, where the number of origins
338 increased to reach a similar frequency as HB and CWT during high runoffs. However, SFP70 is
339 almost twice the size of even the largest watersheds at the other study areas. Additionally,
340 several of the new origins that developed at SFP70 belonged to short reaches in boulder deposits,
341 which explains why wet stream length did not increase rapidly with runoff despite the

342 proliferation of origins. A few origins activated or dried up at HB, PVY, and CWT watersheds,
343 but only at the highest or lowest flows mapped.

344 Network connectivity varied widely at low flows, but generally increased with runoff
345 (Figure 5). All CWT catchments remained highly connected, while the other study areas did not
346 show consistent patterns. Connectivity did not always increase monotonically, as isolated
347 reaches may activate at the extremities of dry tributaries during storms, decreasing the connected
348 proportion of the now more extensive network. For SFP70, maximum connectivity actually
349 occurred at a moderate runoff of 1 mm/day.

350 *4.2 Geomorphic channel metrics*

351 Geomorphic channel heads followed the same trends as flow origins, with fewer heads
352 and larger mean upslope areas for FNW, PVY, and SFP (Table 3). Head density was highest at
353 HB and lowest at SFP. We normalized bankfull width and depth measurements (m) by the
354 logarithm of upslope area ($\log_{10}m^2$) at channel transects to calculate metrics of mean channel
355 width and depth for each catchment (Table 3). Channels were wider at CWT and FNW and
356 slightly deeper at HB. Similar to wet stream length, drainage density of the geomorphic channel
357 was greatest at HB and shortest at FNW and SFP. However, PVY25 and PVY35 had fairly high
358 geomorphic drainage density values despite producing low to moderate wet stream lengths on
359 average. To compare the geomorphic and wet networks, we normalized the geomorphic drainage
360 density by the estimated wet drainage density at exceedance probabilities of 25, 50, and 75%
361 (Table 3). Because wet stream length hardly changed at CWT, all three geomorphic-wet drainage
362 density ratios were near 1. For HB, FNW, and SFP, drainage density of the wet stream
363 approached that of the geomorphic channel between exceedance probabilities of 25 and 50%,
364 although the drainage density ratios remained slightly above 1 at HB25, FNW16, FNW37, and

365 SFP70. Conversely, the ratios were all much greater than 1 at PVY, indicating that the eroded
366 channel extended beyond the normal limits of the wet network. We should emphasize that the
367 locations of the channel and wet stream did not always coincide. For example, we observed that
368 reaches below small seeps at HB contained water at even the driest conditions mapped but did
369 not necessarily have a defined channel bed owing to low flow rates. On the other hand, some
370 reaches that possessed a geomorphic channel almost never carried flow.

371

372

373 *4.3 Rates and correlates of network expansion*

374 Slope values of the power-law function between wet stream length and runoff (β) were
375 quite low for CWT and FNW14 (Table 4). At CWT, we performed one set of mappings at a
376 particularly high flow that surpassed several of the peak floods on record and had an exceedance
377 probability of less than 1% in terms of mean daily flow. Despite the sizeable storm, stream
378 length barely grew (Figure 5). Aside from CWT, β values were highly variable among sites
379 within the same physiographic province. The greatest β values occurred at PVY35, HB25, and
380 PVY25, indicating considerable network expansion and contraction (Table 4).

381 There was a significant negative correlation between bankfull width and β (Table 5). The
382 narrowest channels in our study were at PVY25 and PVY35, which had two of the highest β
383 values. A negative correlation also existed for bankfull depth but was not significant. The
384 geomorphic-wet drainage density ratios were positively correlated to β , so streams that
385 underwent greater changes in length commonly had a geomorphic channel that extended beyond
386 the wet network. β was inversely related to the base flow index (Figure 7). The most significant
387 relationships were for the mean and coefficient of variation of surface network connectivity

388 across mappings. A negative correlation for the mean and positive correlation for the coefficient
389 of variation suggests that networks with highly dynamic lengths had lower surface connectivity.

390

391 **5. Discussion**

392 *5.1 Wet stream length dynamics*

393 Basic rock type strongly correlates with the number and upslope contributing area of flow
394 origins in the study catchments. Sites underlain by sedimentary rock at FNW, PVY, and SFP in
395 the Appalachian Plateau and Valley and Ridge have fewer flow origins with greater upslope
396 areas than catchments with crystalline substrate at HB and CWT (Figure 5). Jaeger et al. (2007)
397 also attribute contrasts in upslope area in the Washington Coast Range to lithology, although, in
398 this case, origins form at smaller source areas in sedimentary rock than in basalt watersheds.

399 Paybins (2003) reports upslope areas of 3 to 18 ha for intermittent flow origins in the
400 Appalachian Plateau, which are comparable but mostly larger than values for FNW. Streams at
401 HB and CWT begin much higher in the watershed at contributing areas of less than 1 ha.
402 Previous work at HB likewise discovered flow initiation at small upslope areas of 0.25 ha or less
403 (Zimmer et al., 2013). However, the mean upslope area values at CWT are an order of magnitude
404 lower than those found by Rivenbark and Jackson (2004) at nearby sites in the Blue Ridge. This
405 study may not have included short reaches below bedrock springs that are common in the Blue
406 Ridge, which could account for the discrepancy.

407 The number of flow origins changes little with runoff, with the exception of SFP70
408 (Figure 5). Whiting and Godsey (2016) also observed relatively stationary origins at their Idaho
409 watersheds, although Godsey and Kirchner (2014) determined that the number of origins
410 increases with runoff according to a power-law function for sites in California. In addition to the

411 distinct regional setting of our study, this disagreement may be due to the exclusion of wet
412 reaches shorter than 10 m by Godsey and Kirchner (2014) to match the available DEM
413 resolution and GPS accuracy. Some of the tributaries at our sites contract to a single pool near
414 the upstream end of the network during dry conditions, as is the case for the southwest branch of
415 PVY35 (Figures 3 and 4), which would otherwise be omitted following the 10 m rule. While
416 such small reaches are inconsequential for some purposes, these locations can serve as habitat
417 refugia (Jaeger and Olden, 2012) and often maintain subsurface connection to downstream
418 waters (Boulton et al., 1998). A small decrease in mean upslope area with increasing runoff
419 accompanies the fairly consistent number of flow origins (Figure 5), signaling that network
420 expansion and contraction mostly proceed by coalescence and disintegration of wet reaches
421 (Bhamjee and Lindsay, 2011; Peirce and Lindsay, 2015) and, to a lesser extent, the migration of
422 origins. Activation and deactivation of entire tributaries typically only occur at short reaches
423 amid boulder fields at SFP70 or during quite wet or dry conditions (exceedance probabilities less
424 than 25% or greater than 75%) at HB, PVY, and CWT (Figure 2).

425 Wet drainage density varies from 0.1 to 11 km/km² at our sites, which corresponds with
426 values found in the western U.S. (Roberts and Klingeman, 1972; Wigington et al., 2005; Godsey
427 and Kirchner, 2014; Whiting and Godsey, 2016), England (Gregory and Walling, 1968; Blyth
428 and Rodda, 1973), and Australia (Day, 1978; Day, 1980). However, Goulsbra et al. (2014)
429 measured a maximum wet drainage density of 30 km/km² in a peatland catchment in England.
430 Stream length has a minor tendency to be highest at HB and CWT (Figure 5), but β slope values
431 reveal more pronounced distinctions between sites (Table 4). The β values for our catchments
432 range from 0.04 to 0.71, which is nearly identical to the range of 0.02 to 0.69 that Godsey and
433 Kirchner (2014) report from the literature. Our project does not characterize the wet network

434 across all seasons, antecedent conditions, or extreme events, so the actual variability is
435 undoubtedly greater. Stream length at CWT remains stable and highly connected for all
436 mappings (Figure 5). Studies show that streams underlain by sedimentary rock generally have
437 shorter flow durations, a wider range of lengths, and more network disconnections than in granite
438 basins (Day, 1980; Whiting and Godsey, 2016). Likewise, streams lengths are less consistent at
439 FNW, PVY, and SFP (Table 4), which lie in sandstones and shales (Table 2), than at CWT.
440 However, the β value at FNW14 is practically the same as those at CWT. Furthermore, the
441 glaciated HB catchments have β values similar to sites in the sedimentary Valley and Ridge and
442 Appalachian Plateau. Thus, factors such as geologic structure and the depth, grain size
443 distribution, and resulting water storage and permeability of surficial material must also
444 influence stream length dynamics. In the case of CWT, the warm, humid climate has weathered
445 deep, permeable soils that are able to transport and store huge volumes of subsurface flow
446 between storms (Hewlett and Hibbert, 1963; Hatcher, 1988) to supply streams with perennial,
447 connected flow.

448 *5.2 Relationship between the geomorphic and wet stream networks*

449 The geomorphic channel matches the wet stream almost exactly at CWT, but geomorphic
450 and wet drainage density values converge at different flows for the remaining study areas (Table
451 3). At HB, FNW, and SFP, the geomorphic and wet drainage densities are nearly equal at
452 moderate-high runoffs between exceedance probabilities of 25 and 50%. The geomorphic
453 channel extends past the mapped wet network at PVY, even for an exceedance probability of
454 25%, instead representing events with longer recurrence intervals. Adams and Spotila (2005)
455 found that channel-forming flows for steep headwater streams without floodplains in the Valley
456 and Ridge have recurrence intervals on the order of decades. Despite residing in the Valley and

457 Ridge, the geomorphic network at SFP70 reflects smaller, more frequent events like at HB and
458 FNW. Both Day (1980) and Jaeger et al. (2007) note that the eroded channel is longer than the
459 wet stream in sedimentary basins, which holds true for FNW, PVY, and SFP for exceedance
460 probabilities greater than 50%. However, drainage density ratios at HB indicate that the
461 geomorphic network is more extensive than the wet stream at these sites as well, even though the
462 substrate is not sedimentary rock.

463 We should be careful to distinguish geomorphic channels and wet streams in research as
464 well as policy, as the relationship between these features is not the same everywhere. Currently,
465 decisions regarding stream networks often depend on the expression of the geomorphic channel.
466 The final ruling of the U.S. Clean Water Act (33 CFR § 328) in 2015 mandates that ephemeral
467 streams lacking physical indicators of flow, including a defined channel bed and banks, are not
468 considered tributaries that fall under federal jurisdiction. While several of the catchments in our
469 study have longer geomorphic networks than the wet stream at most flows, the actual locations
470 of the channel and stream do not always coincide. Channel scouring is more likely where the
471 landscape is locally steep or confined and can concentrate sufficient stream power to erode a bed
472 at high runoffs (Bull, 1979; Taylor and Kite, 2006). On the other hand, we observed some
473 perennial reaches that always carry water but do not have a defined channel. The recurrence
474 interval of channel-forming flows also varies from less than 1 (Powell et al., 2006) to 10s of
475 years (Adams and Spotila, 2005), so geomorphic channels represent floods of different
476 magnitudes. Therefore, we risk misunderstanding the actual range of stream lengths and their
477 associated flow duration by only considering geomorphic channel dimensions.

478 *5.3 Regional versus local geology*

479 Physiographic provinces, which define regions of similar rock type and structure,
480 distinguish sites by the number and source area of flow origins and indicate approximate stream
481 lengths (Figure 5). HB in New England exhibits high wet stream lengths, the greatest density of
482 flow origins, and the smallest upslope areas. Stream length and origin density are moderately
483 high and upslope areas are low at CWT in the Blue Ridge, but network dynamics are minimal.
484 FNW in the Appalachian Plateau and PVY/SFP in the Valley and Ridge produce a small number
485 of flow origins with source areas that are nearly an order of magnitude larger than those at HB
486 and CWT. Despite these trends, the geomorphic networks and wetting and drying patterns of
487 catchments within a single physiographic province reflect local geologic features.

488 PVY and SFP in the Valley and Ridge exemplify the impacts of site-specific geology on
489 channel development. Bedrock consists of nonresistant shales at PVY and highly resistant
490 sandstones at SFP (Table 2). Streams incise extensive networks of deep, V-shaped gullies into
491 the erodible shales underlying PVY (Mills, 1981; Mills et al., 1987); the resulting geomorphic
492 channel is much longer than the wet stream most of the time (Table 3). Geomorphic channel
493 head and drainage density are lower at SFP and are closer to values for FNW in the Appalachian
494 Plateau. A caprock of resistant Keefer and Rose Hill sandstones at SFP weathers into large
495 boulders that fill stream hollows and prevent the downcutting of ravines with steep side slopes
496 that is evident at PVY (Mills, 1981). Such coarse boulder deposits transport water without a need
497 for lengthening surface flow and forming a geomorphic channel. Incidentally, although the
498 geomorphic network is several times longer at PVY than SFP, the channels are narrower in width
499 (Table 3). This observation suggests that PVY and SFP develop unique channel geometries to
500 efficiently remove runoff and sediment according to the underlying rock type.

501 Local lithology additionally correlates to the variability of wet stream length at PVY and
502 SFP. Shales have lower permeability and produce less base flow (Carlston, 1963) than more
503 permeable sandstones. Smaller proportions of base flow in impermeable geology increase the
504 likelihood that streams will contract or dry up (Winter, 2007) and create a higher eroded drainage
505 density, owing to the predominance of quick runoff (Carlston, 1963). Our results similarly show
506 that wet stream length has greater and more consistent flow duration with lower β values at SFP
507 than at PVY (Figures 3 and 4; Table 4) and that the geomorphic channel is shorter. Kowall
508 (1976) and Paybins (2003) also report greater, less variable summer low flows and a greater
509 chance of perennial flow in basins underlain by sandstone rather than siltstone and shale. The
510 significant inverse relationship between the base flow index and β (Figure 7) further indicates
511 that flashier streams with a lower proportion of base flow experience more network dynamics.

512 Geologic structure provides another potential control on stream length dynamics. PVY is
513 located on the scarp slope of a homoclinal ridge and cross-cuts various bedding planes, creating
514 secondary permeability in an otherwise relatively impermeable shale. The alternation of strata
515 along a scarp slope produces opportunities for water to discharge from or infiltrate into the rock,
516 depending on the porosity and permeability of the geologic layer. We observed that the sequence
517 of high and low flow duration reaches along the PVY25 and PVY35 tributaries (Figure 3) largely
518 follows local valley width, which can vary as a function of lithofacies resistance (Taylor and
519 Kite, 2006). Valley confinement also explains patterns of network contraction in desert streams
520 examined by Stanley et al. (1997), with wide, unconstrained reaches drying first. The bands of
521 low flow duration in PVY25 occur at the same relative watershed position in all three tributaries,
522 possibly corresponding to distinct stratigraphic layers within the shale and sandstone units
523 exposed on the scarp slope. SFP and FNW, on the other hand, are on the dip slopes of folds.

524 These catchments remain more connected and have greater flow durations than PVY conceivably
525 because, in part, the streams flow along the top of the strata rather than across multiple layers.
526 Further research at additional sites is necessary to better quantify the impacts of lithology versus
527 structure on wet stream length.

528 Subwatershed-scale geology may explain discrepancies in β values that are also notable
529 between catchments in other study areas. For example, the β value at HB25 is two to three times
530 that of the other HB sites (Table 4). The till deposits overlying the bedrock at HB are
531 heterogeneous in terms of depth (reaching 5-8 m in HB42; Benettin et al., 2015), grain size, and
532 sorting. Boulder deposits are a common feature of poorly-sorted glacial material and are present
533 in much of HB25 as well as the southeastern section of HB42, where streams are short and
534 disconnected (Figure 3). Deep or coarse surficial material transmits water easily in the
535 subsurface and may reduce the need for surface flow at low runoffs, which would account for the
536 higher β value. Nonetheless, the inherent spatial heterogeneity of glacial till decreases the
537 predictability of stream length dynamics, as is also evident from the large variation in flow origin
538 density at HB in comparison to the other study areas (Figure 6).

539 As Costigan et al. (2016) describe, flow permanence is a function of geologic attributes
540 operating at spatial scales ranging from sediment particles to watersheds. Consideration of
541 geology at all scales is essential to comprehensively characterize stream intermittency. Because
542 of the time and expense associated with data collection, understanding the information available
543 at each scale can help focus efforts for a particular research question or management goal. Our
544 work suggests that larger physiographic regions or basic rock type (e.g., sedimentary or
545 crystalline) may be sufficient to estimate the relative frequency and mean upslope area of flow
546 origins. To approximate the degree of network expansion and contraction in a catchment,

547 knowledge of the lithology and structure may be necessary. More detailed mapping of lithofacies
548 and surficial material can locate specific stream disconnections. The appropriate scale of analysis
549 ultimately depends on the informational needs of a particular project.

550 *5.4 Predictors of stream length variability*

551 Repeated stream mappings and thorough geologic characterization are essential to
552 accurately represent the length and flow duration of headwaters. However, field mapping is time-
553 intensive, and high resolution geologic maps are not always available. Forgoing these data, we
554 found that fairly simple measurements can serve as useful proxies of network dynamics. The
555 negative correlation between bankfull width and β (Table 5) demonstrates that wide channels are
556 able to accommodate a huge range of flows without needing to lengthen. CWT and FNW have
557 the widest channels in our study, although Day (1980) observed that channels are usually wider
558 in crystalline granite than in sedimentary basins. Bankfull width is easy to measure and compare
559 between catchments as a first approximation of stream length variability.

560 Streams with less base flow and a geomorphic channel that extends past the wet network
561 most of the time undergo greater changes in length. Calculation of the base flow index from
562 discharge data is simple, objective, and can be performed remotely. Base flow proportions do
563 vary with watershed size, but a regional base flow index can be estimated from USGS gauges.
564 Finally, surface connectivity of the wet stream is the most significant indicator of network
565 expansion and contraction. Streams with low mean connectivity also tend to have the most
566 variable connectivity and extreme length dynamics. Thus, although these streams are more
567 disconnected on average, the flow becomes nearly continuous during wet conditions. Such
568 catchments have the potential to provide a greater diversity of landscape functions than networks
569 that remain mostly connected at all times, like CWT. Stream mapping is the most reliable, albeit

570 time-consuming, method to determine network connectivity, although unmanned aerial vehicles
571 and other technologies may ease this burden in the future (Spence and Mengistu, 2016).

572

573 **6. Conclusion**

574 Our results demonstrate that wet stream length in headwaters varies regionally by
575 physiographic province. New England and the Blue Ridge have high stream length and flow
576 origin density, although the Blue Ridge streams remain mostly connected and undergo far less
577 expansion and contraction than the remaining study areas. In comparison, catchments in the
578 Appalachian Plateau and Valley and Ridge have fewer flow origins with much larger drainage
579 areas than in the other two provinces. Site lithology, geologic structure, and surficial materials
580 superimpose additional controls on headwater behavior. For example, shale bedrock on a scarp
581 slope corresponds to lower flow duration, a more extensively eroded geomorphic channel
582 network, and higher coefficients describing the degree of network expansion with increasing
583 runoff (β) than for sandstone catchments in the same Valley and Ridge province. Transmissive
584 surficial deposits of coarse boulders or deep sediment valley fills reduce the need for surface
585 flow and coincide with stream disconnections. Simple measurements permit an approximation of
586 β values, as streams with wide channels, more base flow, high surface connectivity, and little
587 difference between the geomorphic and wet stream networks change less in length with runoff.

588 Stream mapping is labor-intensive and usually limited to small areas. Forgoing field
589 surveys of all headwaters, some level of generalization by geographic region, climate zone,
590 geologic unit, or land cover class is necessary to inform watershed management. However,
591 traditional divisions may not suffice for the optimum classification of headwaters. For example,
592 the Appalachian Mountains are often considered a single entity, but β values from our study span

593 the entire range of those reported in the literature from catchments around the world. More data
594 on wet stream length in distinct locations will help inform the appropriate criteria and scale by
595 which to categorize headwaters for various policy initiatives. Our study only examines forested
596 watersheds, so other factors likely influence stream wetting and drying in agricultural and urban
597 environments. In addition to obvious relevance for surface water policy, this and similar work
598 has implications for mass fluxes of sediment and solutes from headwaters, organism dispersal
599 and refugia, biogeochemical transformations, and furthering our understanding of the processes
600 that generate surface flow in watersheds.

601

602 **Supporting information**

603 Figure S1. HB13; Figure S2. HB25; Figure S3. HB42; Figure S4. FNW14; Figure S5. FNW16;
604 Figure S6. FNW37; Figure S7. PVY25; Figure S8. PVY35; Figure S9. SFP70; Figure S10.
605 CWT12; Figure S11. CWT33; Figure S12. CWT40

606

607 **References**

- 608 Abrahams, A. D. (1984). Channel networks: a geomorphological perspective. *Water Resources*
609 *Research*, 20, 161-188.
- 610 Acuña, V., Datry, T., Marshall, J., Barceló, D., Dahm, C. N., Ginebreda, A., ... & Palmer, M. A.
611 (2014). Why should we care about temporary waterways?. *Science*, 343, 1080-1081.
- 612 Adams, M. B., Kochenderfer, J. N., Wood, F., Angradi, T. R., & Edwards, P. (1994). Forty years
613 of hydrometeorological data from the Fernow Experimental Forest, West Virginia. U.S.
614 Department of Agriculture, Forest Service, Northeastern Forest Experiment Station.
- 615 Adams, R. K., & Spotila, J. A. (2005). The form and function of headwater streams based on

616 field and modeling investigations in the Southern Appalachian Mountains. *Earth Surface*
617 *Processes and Landforms*, 30, 1521-1546.

618 Adams, M. B., Edwards, P. J., Ford, W. M., Schuler, T. M., Thomas-Van Gundy, M., & Wood,
619 F. (2012). Fernow Experimental Forest: research history and opportunities. U.S.
620 Department of Agriculture, Forest Service, Experimental Forests and Ranges.

621 Alexander, R. B., Boyer, E. W., Smith, R. A., Schwarz, G. E., & Moore, R. B. (2007). The role
622 of headwater streams in downstream water quality. *Journal of the American Water*
623 *Resources Association*, 43, 41-59.

624 Bailey, A. S., Hornbeck, J. W., Campbell, J. L., & Eagar, C. (2003). Hydrometeorological
625 database for Hubbard Brook Experimental Forest: 1955-2000, 305. U.S. Department of
626 Agriculture, Forest Service, Northeastern Research Station.

627 Bailey, S. W., Buso, D. C., & Likens, G. E. (2003). Implications of sodium mass balance for
628 interpreting the calcium cycle of a forested ecosystem. *Ecology*, 84, 471-484.

629 Barton, C.C. (1997). Bedrock geologic map of Hubbard Brook Experimental Forest and maps of
630 fractures and geology in roadcuts along Interstate 93, Grafton County, New Hampshire,
631 Scale 1:2000. U.S. Geological Survey Miscellaneous Investigation Series I-2562.

632 Benettin, P., Bailey, S. W., Campbell, J. L., Green, M. B., Rinaldo, A., Likens, G. E., McGuire,
633 K. J., & Botter, G. (2015). Linking water age and solute dynamics in streamflow at the
634 Hubbard Brook Experimental Forest, NH, USA. *Water Resources Research*, 51, 9256–
635 9272.

636 Bhamjee, R., & Lindsay, J. B. (2011). Ephemeral stream sensor design using state loggers.
637 *Hydrology and Earth System Sciences*, 15, 1009-1021.

638 Bishop, K., Buffam, I., Erlandsson, M., Fölster, J., Laudon, H., Seibert, J., & Temnerud, J.

639 (2008). Aqua Incognita: The unknown headwaters. *Hydrological Processes*, 22, 1239-
640 1242.

641 Blasch, K. W., Ferré, T., Christensen, A. H., & Hoffmann, J. P. (2002). New field method to
642 determine streamflow timing using electrical resistance sensors. *Vadose Zone Journal*, 1,
643 289-299.

644 Blinn, C. R., & Kilgore, M. A. (2001) Riparian management practices: a summary of state
645 guidelines. *Journal of Forestry*, 99, 11-17.

646 Blyth, K., & Rodda, J. C. (1973). A stream length study. *Water Resources Research*, 9, 1454-
647 1461.

648 Boulton, A. J., Findlay, S., Marmonier, P., Stanley, E. H., & Valett, H. M. (1998). The functional
649 significance of the hyporheic zone in streams and rivers. *Annual Review of Ecology and*
650 *Systematics*, 29, 59-81.

651 Brooks, R. T., & Colburn, E. A. (2011). Extent and channel morphology of unmapped headwater
652 stream segments of the Quabbin watershed, Massachusetts. *Journal of the American*
653 *Water Resources Association*, 47, 158-168.

654 Bull, W. B. (1979). Threshold of critical power in streams. *Geological Society of American*
655 *Bulletin*, 90, 453-464.

656 Buttle, J. M., Boon, S., Peters, D. L., Spence, C., van Meerveld, H. J., & Whitfield, P. H. (2012).
657 An overview of temporary stream hydrology in Canada. *Canadian Water Resources*
658 *Journal*, 37, 279-310.

659 Calkins, D., & Dunne, T. (1970). A salt tracing method for measuring channel velocities in small
660 mountain streams. *Journal of Hydrology*, 11, 379-392.

661 Calver, A. (1990). Stream head migration: an indicator of runoff processes on chalklands.

662 *Catena*, 17, 399-408.

663 Cardwell, D.H., Erwin, R.B., & Woodward, H.P. (1968) Geologic map of West Virginia, 2
664 sheets, Scale 1:250,000. West Virginia Geological and Economic Survey.

665 Carlston, C. W. (1963). Drainage density and streamflow. U.S. Geological Survey Professional
666 Paper 422-C.

667 Chapin, T. P., Todd, A. S., & Zeigler, M. P. (2014). Robust, low-cost data loggers for stream
668 temperature, flow intermittency, and relative conductivity monitoring. *Water Resources*
669 *Research*, 50, 6542-6548.

670 Cohen, M. J., Creed, I. F., Alexander, L., Basu, N. B., Calhoun, A. J., Craft, C., ... & Jawitz, J.
671 W. (2016). Do geographically isolated wetlands influence landscape functions?
672 *Proceedings of the National Academy of Sciences*, 113, 1978-1986.

673 Costigan, K. H., Jaeger, K. L., Goss, C. W., Fritz, K. M., & Goebel, P. C. (2016). Understanding
674 controls on flow permanence in intermittent rivers to aid ecological research: integrating
675 meteorology, geology and land cover. *Ecohydrology*, 9, 1141-1153.

676 Datry, T., Larned, S. T., & Tockner, K. (2014). Intermittent rivers: a challenge for freshwater
677 ecology. *Bioscience*, 64, 229-235.

678 Day, D. G. (1978). Drainage density changes during rainfall. *Earth Surface Processes*, 3, 319-
679 326.

680 Day, D. G. (1980). Lithologic controls of drainage density: A study of six small rural catchments
681 in New England, NSW. *Catena*, 7, 339-351.

682 De Vries, J. J. (1994). Dynamics of the interface between streams and groundwater systems in
683 lowland areas, with reference to stream net evolution. *Journal of Hydrology*, 155, 39-56.

684 Dietrich, W. E., & Dunne, T. (1993). The channel head. In K. J. Beven, & M. J. Kirkby (Eds.),

685 *Channel Network Hydrology* (pp. 175-219). Chichester, UK: John Wiley & Sons.

686 Doyle, M. W., & Bernhardt, E. S. (2010). What is a stream?. *Environmental Science*
687 *& Technology, 45*, 354-359.

688 Dunne, T., & Leopold, L. B. (1978). *Water in Environmental Planning*. San Francisco, CA: W.
689 H. Freeman and Company.

690 Fritz, K. M., Hagenbuch, E., D'Amico, E., Reif, M., Wigington, P. J., Leibowitz, S. G., ... &
691 Nadeau, T. L. (2013). Comparing the extent and permanence of headwater streams from
692 two field surveys to values from hydrographic databases and maps. *Journal of the*
693 *American Water Resources Association, 49*, 867-882.

694 Godsey, S. E., & Kirchner, J. W. (2014). Dynamic, discontinuous stream networks:
695 Hydrologically driven variations in active drainage density, flowing channels and stream
696 order. *Hydrological Processes, 28*, 5791-5803.

697 Goulsbra, C., Evans, M., & Lindsay, J. (2014). Temporary streams in a peatland catchment:
698 pattern, timing, and controls on stream network expansion and contraction. *Earth Surface*
699 *Processes and Landforms, 39*, 790-803.

700 Granato, G. E. (2009). Computer programs for obtaining and analyzing daily mean stream flow
701 data from the U.S. Geological Survey National Water Information System Web Site. U.S.
702 Geological Survey Open-File Report 2008-1362.

703 Gregory, K. J., & Walling, D. E. (1968). The variation of drainage density within a catchment.
704 *Hydrological Sciences Journal, 13*, 61-68.

705 Hadley, R. F., & Schumm, S. A. (1961). Sediment sources and drainage basin characteristics in
706 upper Cheyenne River basin. U.S. Geological Survey Water-Supply Paper 1531-B, 137-
707 198.

708 Hatcher Jr., R. D. (1988). Bedrock geology and regional geologic setting of Coweeta Hydrologic
709 Laboratory in the eastern Blue Ridge. In W. T. Swank, & D. A. Crossley Jr. (Eds),
710 *Ecological Studies: Forest Hydrology and Ecology at Coweeta* (Vol. 66, pp. 81-92). New
711 York, NY: Springer-Verlag.

712 Hedman, E. R., & Osterkamp, W. R. (1982). Streamflow characteristics related to channel
713 geometry of streams in western United States. U.S. Geological Survey Water Supply
714 Paper 2193.

715 Hewlett, J. D., & Hibbert, A. R. (1963). Moisture and energy conditions within a sloping soil
716 mass during drainage. *Journal of Geophysical Research*, 68, 1081-1087.

717 Hewlett, J. D., & Hibbert, A. R. (1967). Factors affecting the response of small watersheds to
718 precipitation in humid areas. *Forest Hydrology*, 1, 275-290.

719 Jaeger, K. L., Montgomery, D. R., & Bolton, S. M. (2007). Channel and perennial flow initiation
720 in headwater streams: management implications of variability in source-area size.
721 *Environmental Management*, 40, 775-786.

722 Jaeger, K. L., & Olden, J. D. (2012). Electrical resistance sensor arrays as a means to quantify
723 longitudinal connectivity of rivers. *River Research and Applications*, 28, 1843-1852.

724 Kowall, S. J. (1976). The hypsometric integral and low streamflow in two Pennsylvania
725 provinces. *Water Resources Research*, 12, 497-502.

726 Larned, S. T., Datry, T., Arscott, D. B., & Tockner, K. (2010). Emerging concepts in temporary-
727 river ecology. *Freshwater Biology*, 55, 717-738.

728 Laseter, S. H., Ford, C. R., Vose, J. M., & Swift, L. W. (2012). Long-term temperature and
729 precipitation trends at the Coweeta Hydrologic Laboratory, Otto, North Carolina, USA.
730 *Hydrology Research*, 43, 890-901.

731 Lyne, V., & Hollick, M. (1979). Stochastic time-variable rainfall-runoff modelling. In
732 *Proceedings of the Hydrology and Water Resources Symposium* (Vol. 79/10, pp. 89-93).
733 Institute of Engineers Australia National Conference.

734 Mills, H. H. (1981). Boulder deposits and the retreat of mountain slopes, or, " gully gravure"
735 revisited. *The Journal of Geology*, 89, 649-660.

736 Mills, H. H., Brakenridge, G. R., Jacobson, R. B., Newell, W. L., Pavich, M. J., & Pomeroy, J. S.
737 (1987). Appalachian mountains and plateaus. In W. L. Graf (Ed.), *Geomorphic Systems*
738 *of North America* (Centennial Special, Vol. 2, pp. 5-50). Boulder, CO: Geological
739 Society of America.

740 Morgan, R. P. C. (1972). Observations on factors affecting the behaviour of a first-order stream.
741 *Transactions of the Institute of British Geographers*, 56, 171-185.

742 Nadeau, T. L., and Rains, M. C. (2007). Hydrological connectivity between headwater streams
743 and downstream waters: how science can inform policy. *Journal of the American Water*
744 *Resources Associations*, 43, 118-133.

745 National Research Council. (2002). Riparian areas: functions and strategies for management.
746 National Academies Press.

747 Paybins, K. S. (2003). Flow origin, drainage area, and hydrologic characteristics for headwater
748 streams in the mountaintop coal-mining region of southern West Virginia, 2000-01. U.S.
749 Geological Survey.

750 Peirce, S. E., & Lindsay, J. B. (2015). Characterizing ephemeral streams in a southern Ontario
751 watershed using electrical resistance sensors. *Hydrological Processes*, 29, 103-111.

752 Powell, G. E., Mecklenburg, D., & Ward, A. (2006). Evaluating channel-forming discharges: a
753 study of large rivers in Ohio. *Transactions of the ASABE*, 49, 35-46.

754 Price, J. R., Velbel, M. A., & Patino, L. C. (2005). Rates and time scales of clay-mineral
755 formation by weathering in saprolitic regoliths of the southern Appalachians from
756 geochemical mass balance. *Geological Society of America Bulletin*, 117, 783-794.

757 Rivenbark, B. L., & Jackson, C. R. (2004). Average discharge, perennial flow initiation, and
758 channel initiation-small Southern Appalachian basins. *Journal of the American Water*
759 *Resources Association*, 40, 639-646.

760 Roberts, M. C., & Klingeman, P. C. (1972). The relationship of drainage net fluctuation and
761 discharge. Proceedings of the 22nd International Geographical Congress, Canada, 181-
762 91.

763 Russell, P. P., Gale, S. M., Muñoz, B., Dorney, J. R., & Rubino, M. J. (2015). A spatially explicit
764 model for mapping headwater streams. *Journal of the American Water Resources*
765 *Association*, 51, 226-239.

766 Schultz, A. P., Stanley, C. B., Gathright II, T. M., Rader, E. K., Bartholomew, M. J., Lewis, S.
767 E., & Evans, N. H. (1986). Geologic map of Giles County, Virginia, Scale 1:50,000.
768 Virginia Division of Mineral Resources.

769 Seibert, J., & McGlynn, B. L. (2007). A new triangular multiple flow direction algorithm for
770 computing upslope areas from gridded digital elevation models. *Water Resources*
771 *Research*, 43(4).

772 Shaw, S. B. (2016). Investigating the linkage between streamflow recession rates and channel
773 network contraction in a mesoscale catchment in New York State. *Hydrological*
774 *Processes*, 30, 479-492.

775 Skoulikidis, N. T., Sabater, S., Datry, T., Morais, M. M., Buffagni, A., Dörflinger, G., ... &

776 Rosado, J. (2017). Non-perennial Mediterranean rivers in Europe: status, pressures, and
777 challenges for research and management. *Science of The Total Environment*, 577, 1-18.

778 The Southeast Regional Climate Center (SERCC) (2012). Historical Climate Summaries for
779 Virginia. http://www.sercc.com/climateinfo/historical/historical_va.html.

780 Spence, C., & Mengistu, S. (2016). Deployment of an unmanned aerial system to assist in
781 mapping an intermittent stream. *Hydrological Processes*, 30, 493-500.

782 Stanley, E. H., Fisher, S. G., & Grimm, N. B. (1997). Ecosystem expansion and contraction in
783 streams. *Bioscience*, 47, 427-435.

784 Steward, A. L., von Schiller, D., Tockner, K., Marshall, J. C., & Bunn, S. E. (2012). When the
785 river runs dry: Human and ecological values of dry riverbeds. *Frontiers in Ecology and*
786 *the Environment*, 10, 202-209.

787 Taylor, S. B., & Kite, J. S. (2006). Comparative geomorphic analysis of surficial deposits at
788 three central Appalachian watersheds: Implications for controls on sediment-transport
789 efficiency. *Geomorphology*, 78, 22-43.

790 Virginia Division of Mineral Resources. (1993). Geologic Map of Virginia, Scale 1:500,000.
791 Virginia Division of Mineral Resources.

792 Wang, L., & Liu, H. (2006). An efficient method for identifying and filling surface depressions
793 in digital elevation models for hydrologic analysis and modelling. *International Journal*
794 *of Geographical Information Science*, 20, 193-213.

795 Wharton, G. (1994). Progress in the use of drainage network indices for rainfall-runoff modelling
796 and runoff prediction. *Progress in Physical Geography*, 18, 539-557.

797 Whiting, J. A., & Godsey, S. E. (2016). Discontinuous headwater stream networks with stable
798 flowheads, Salmon River Basin, Idaho. *Hydrological Processes*, 30, 2305-2316.

799 Wigington, P. J., Moser, T. J., & Lindeman, D. R. (2005). Stream network expansion: a riparian
800 water quality factor. *Hydrological Processes*, 19, 1715-1721.

801 Winter, T. C. (2007). The role of ground water in generating streamflow in headwater areas and
802 in maintaining base flow. *Journal of the American Water Resources Association*, 43, 15-
803 25.

804 Zimmer, M. A., Bailey, S. W., McGuire, K. J., & Bullen, T. D. (2013). Fine scale variations of
805 surface water chemistry in an ephemeral to perennial drainage network. *Hydrological*
806 *Processes*, 27, 3438-3451.

807 Zimmer, M. A., & McGlynn, B. L. (2017). Ephemeral and intermittent runoff generation
808 processes in a low relief, highly weathered catchment. *Water Resources Research*, doi:
809 10.1002/2016WR019742.

810

811 **Acknowledgements**

812 This study was supported by the National Science Foundation under grant LTER DEB 1114804,
813 the Consortium of Universities for the Advancement of Hydrologic Science Pathfinder
814 Fellowship, and the Cunningham Graduate Fellowship and Graduate Student Association
815 Graduate Research Development Fund Award at Virginia Tech. Fernow and Hubbard Brook
816 Experimental Forests and Coweeta Hydrologic Laboratory are operated and maintained by the
817 U.S. Forest Service. We are grateful to the George Washington and Jefferson National Forests
818 for their cooperation and participation in the project. We would also like to thank Dylan Coward,
819 Jake Diamond, Dave Jensen, Joe Famularo, and Morgan Schulte for assistance in the field as
820 well as two anonymous reviewers for helpful suggestions that improved the manuscript.

821

822

823

824

825

826

827 Table I. Average climatic attributes of the four study areas.

Study area	Mean January/July temperature (°C)	Mean annual precipitation (cm)	Snowfall (% of precipitation)	Reference
HB	-9/18	140	33	Bailey, A. et al. (2003)
FNW	-3/20	146	15	Adams et al. (1994); Adams et al. (2012)
PVY/SFP	-1/22	100	5	SERCC (2012) (Blacksburg, Radford, and Staffordsville)
CWT	3/21	179	2	Laseter et al. (2012)

828

829

830 Table II. Characteristics of the study catchments.

Physiographic province	Study area	Site name ^a (watershed number ^b)	Latitude (°N), Longitude (°W)	Drainage area ^c (ha)	Aspect	Mean elevation ^c (m)	Mean slope ^c (%)	Geology
New England	HB	HB13 (WS 6)	43.95, 71.74	13.4	SE	690	28	schist, granulite
		HB25	43.93, 71.77	25.1	NW	740	28	schist, granulite
		HB42 (WS 3)	43.96, 71.72	42.4	S	632	28	schist, granulite
Appalachian Plateau	FNW	FNW14 (WS 13)	39.06, 79.70	13.9	NE	773	32	shale, sandstone
		FNW16 (WS 10)	39.05, 79.68	15.7	SW	767	31	shale, sandstone
		FNW37 (WS 4)	39.05, 79.69	36.6	SE	822	22	shale, sandstone
Valley and Ridge	PVY	PVY25	37.28, 80.46	25	NW	750	32	shale, sandstone
		PVY35	37.26, 80.48	34.8	N	729	35	shale, sandstone
	SFP	SFP70	37.45, 80.49	69.9	S	1029	27	sandstone
Blue Ridge	CWT	CWT12 (WS 18)	35.05, 83.44	12.4	NW	823	53	gneiss, amphibolite
		CWT33 (WS 34)	35.06, 83.45	32.7	SE	1019	51	gneiss, amphibolite
		CWT40 (WS 32)	35.05, 83.46	39.6	E	1052	44	gneiss

^aNumbers in site name correspond to the drainage area in hectares

^bIf applicable, for gauged catchments at the experimental forests with a designated watershed number

^cAs determined from 3 m DEMs

831

832

833

834

835

836 Table III. Geomorphic channel attributes and geomorphic-wet drainage density ratios.

Site	Mean UA ^a (ha)	Channel head density (heads/km ²)	Mean bankfull width/UA (m/log ₁₀ m ²)	Mean bankfull depth/UA (m/log ₁₀ m ²)	DD ^b (km/km ²)	DD ^b /75 ^c	DD ^b /50 ^c	DD ^b /25 ^c
HB13	0.25	67.11	0.31	0.08	8.65	1.21	1.04	0.90
HB25	0.37	39.81	0.32	0.05	6.65	2.85	1.73	1.05
HB42	0.51	40.12	0.31	0.05	6.68	1.44	1.12	0.92
FNW14	1.14	14.43	0.54	0.06	2.74	1.14	1.05	0.97
FNW16	3.93	6.37	0.42	0.04	2.29	1.96	1.38	1.06
FNW37	2.57	8.19	0.38	0.05	2.43	1.81	1.39	1.13
PVY25	0.82	15.97	0.27	0.05	6.79	6.82	3.65	1.95
PVY35	2.13	11.49	0.24	0.03	4.91	41.49	11.89	3.41
SFP70	3.90	5.72	0.33	0.04	1.67	1.56	1.28	1.05
CWT12	0.91	32.35	0.42	0.04	5.10	1.06	0.98	0.92
CWT33	0.47	15.30	0.33	0.05	3.06	0.99	0.96	0.93
CWT40	0.37	27.76	0.47	0.04	4.72	1.03	1.00	0.98

^aUpslope area (Seibert and McGlynn, 2007) of the geomorphic channel heads

^bDrainage density of the geomorphic network

^cWet drainage density associated with the 25, 50, and 75% exceedance probabilities (km/km²)

837

838

839

840

841

842 Table IV. β (\pm standard error) and the associated R^2 values of the power-law function between
 843 wet stream length and runoff for each site.

Site	β	R^2
HB13	0.15 (± 0.020)	0.92
HB25	0.59 (± 0.033)	0.98
HB42	0.24 (± 0.023)	0.95
FNW14	0.06 (± 0.004)	0.97
FNW16	0.26 (± 0.043)	0.88
FNW37	0.18 (± 0.017)	0.96
PVY25	0.43 (± 0.020)	0.99
PVY35	0.71 (± 0.065)	0.96
SFP70	0.14 (± 0.006)	0.99
CWT12	0.08 (± 0.016)	0.84
CWT33	0.04 (± 0.006)	0.91
CWT40	0.04 (± 0.008)	0.82

844

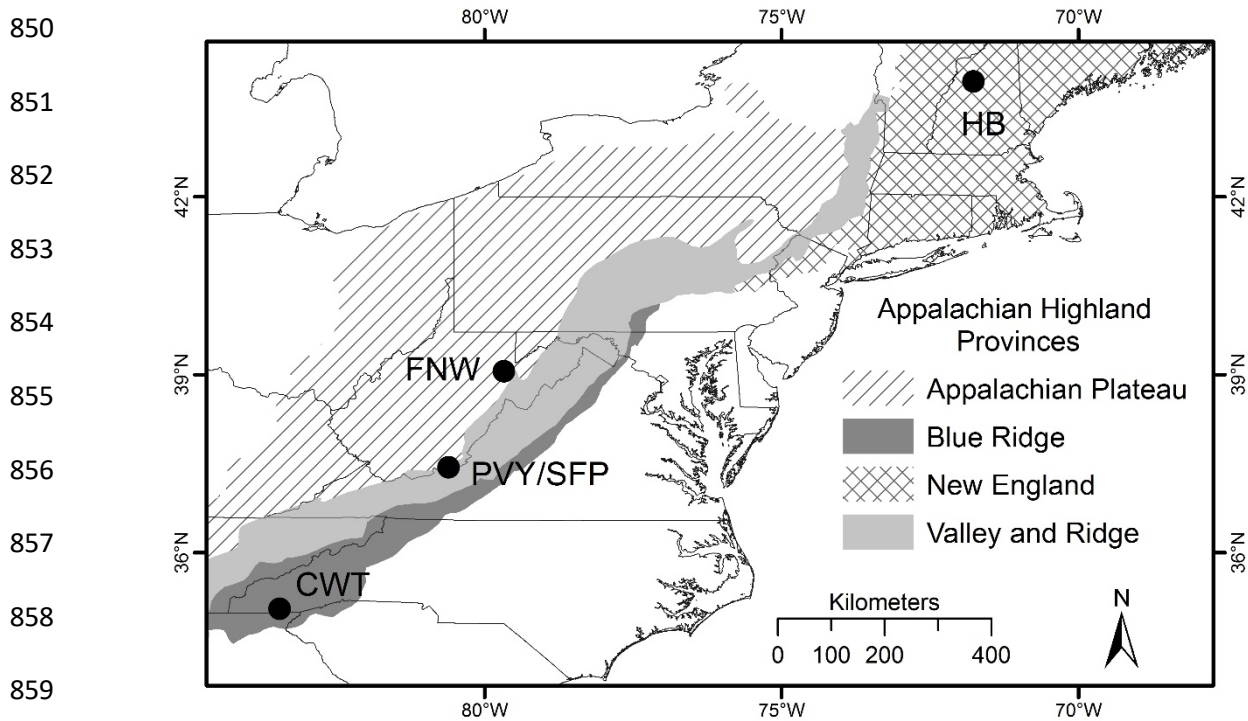
845

846 Table V. Pearson correlations (r) between variables and β . Bold indicates significance at $p =$
 847 0.05. See Table III for abbreviations.

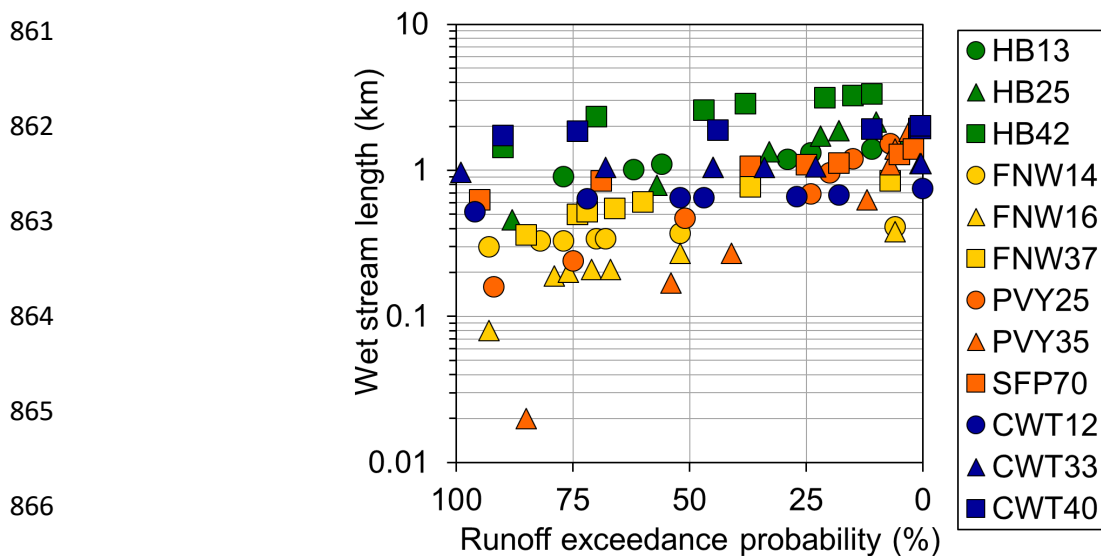
Variable	r
Mean UA (ha)	0.35
Channel head density (heads/km ²)	-0.05
Mean bankfull width/UA (m/m ²)	-0.65
Mean bankfull depth/UA (m/m ²)	-0.19
DD (km/km ²)	0.33
DD/75	0.73
DD/50	0.76
DD/25	0.76
Base flow index (Lyne and Hollick, 1979)	-0.69
Network connectivity—mean	-0.88
Network connectivity—coefficient of variation	0.92

848

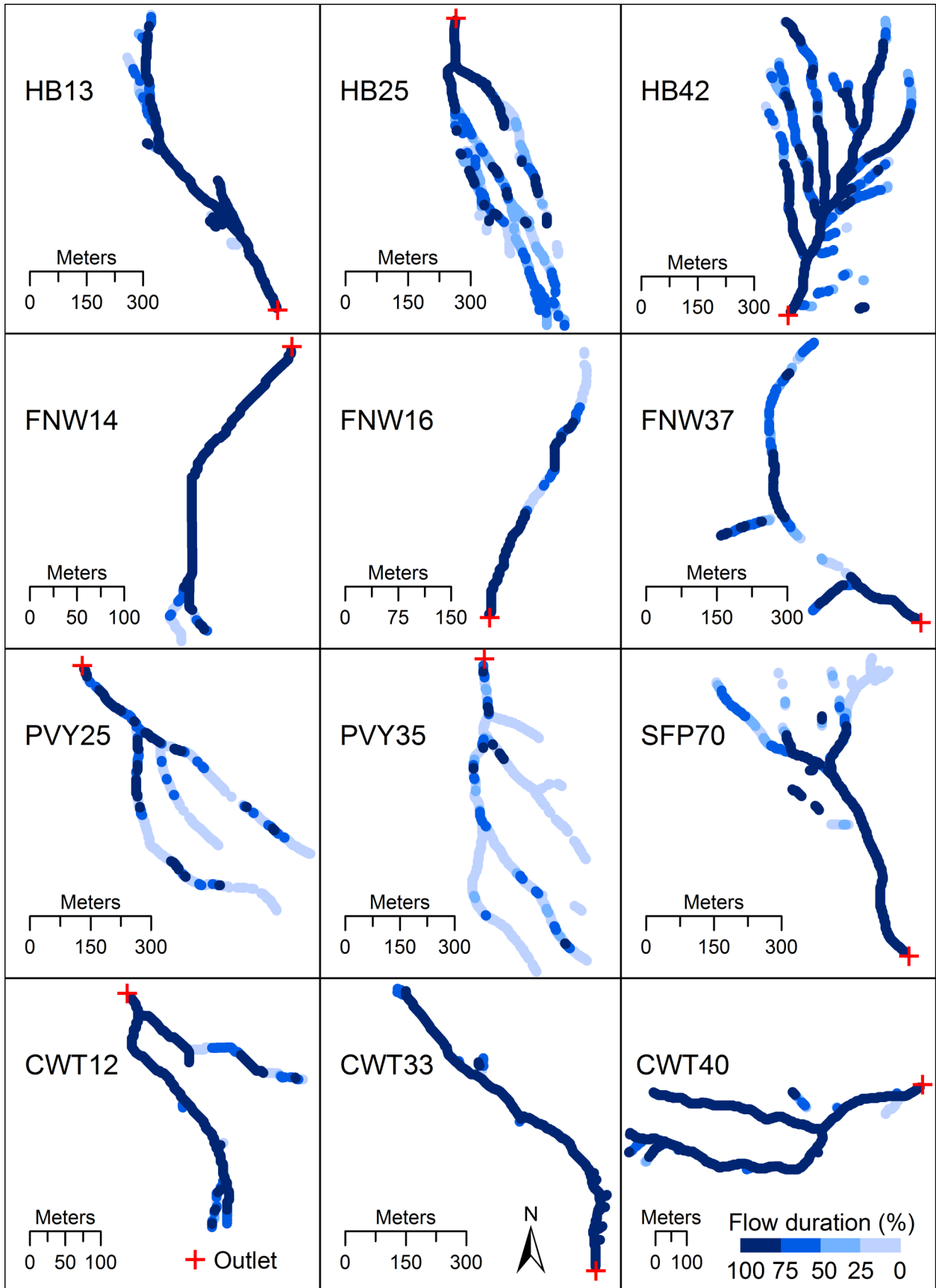
849

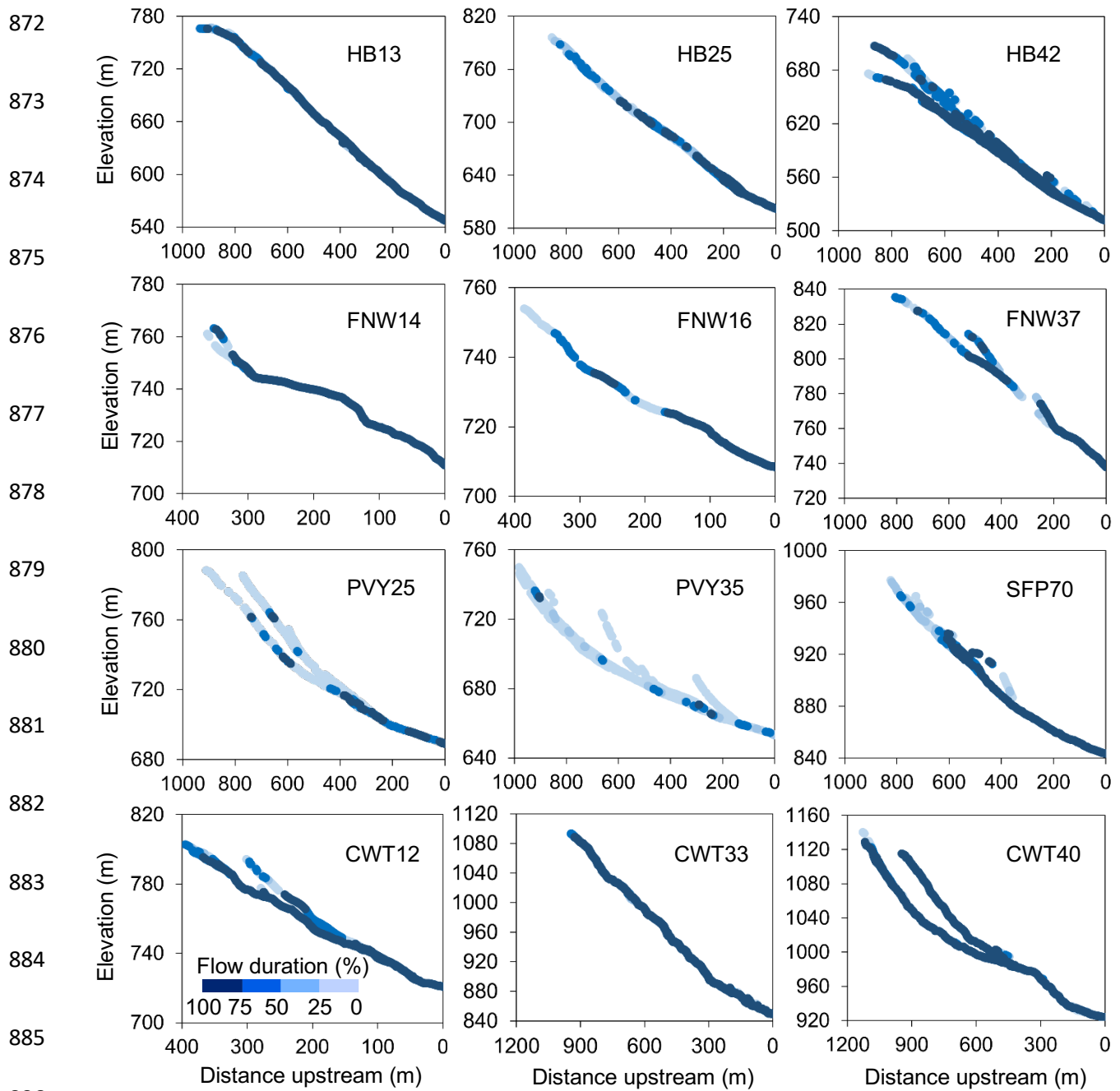


860 Figure 1. Study areas.



867 Figure 2. Wet stream length versus the exceedance probability of the runoff for each mapping, as
 868 determined from flow duration curves of mean daily flow from 2006-2015. Colors correspond to
 869 physiographic province: green for New England, yellow for Appalachian Plateau, orange for
 870 Valley and Ridge, blue for Blue Ridge.



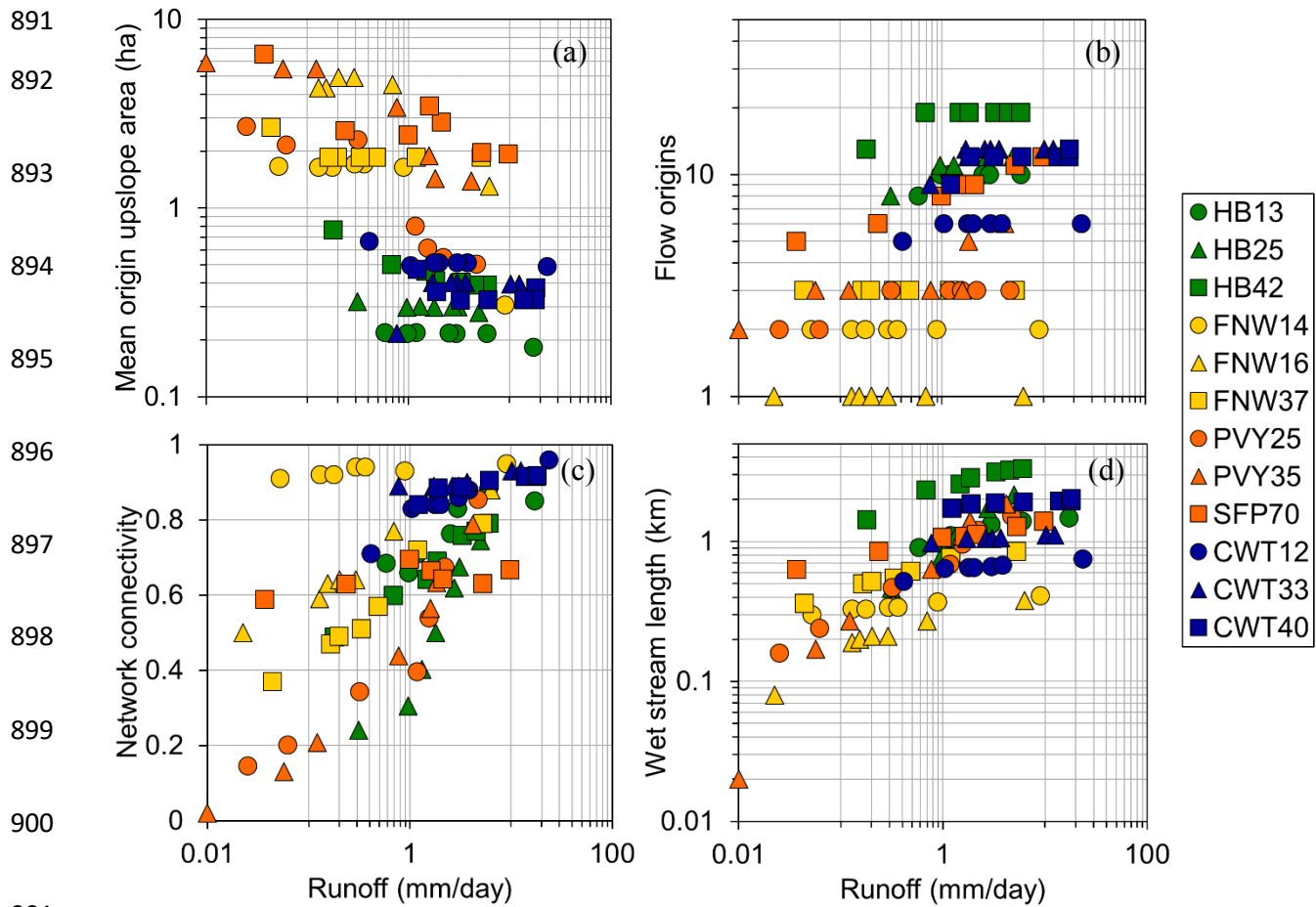


887 Figure 3. Planform view of the wet stream network.

888 Figure 4. Longitudinal profiles of the wet stream network.

889

890



902 Figure 5. Mean upslope area of flow origins (a), number of flow origins (b), network surface
 903 connectivity (c), and wet stream length (d) versus runoff for each mapping. Color scheme same
 904 as Figure 2.

905

906

907

908

909

910
911
912
913
914
915
916
917
918
919
920
921
922
923
924
925
926
927
928

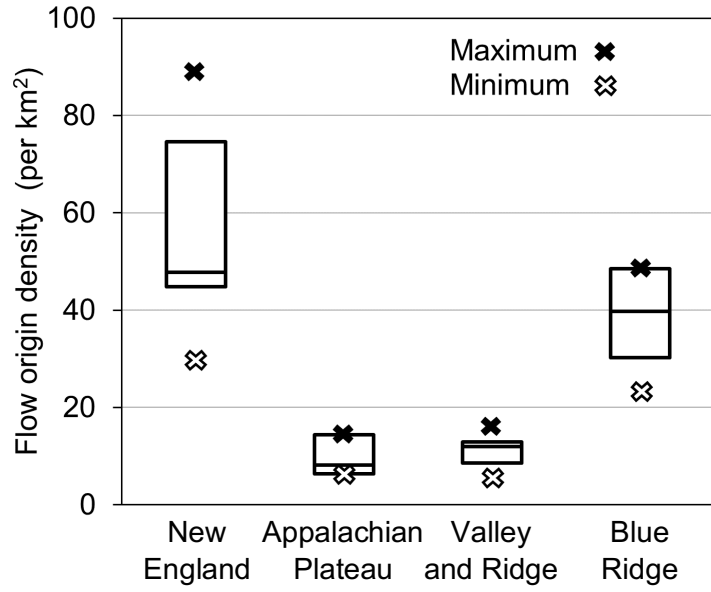


Figure 6. Flow origin density by physiographic province. Each box plot represents data from 21 mappings (3 catchments in each province; 7 mappings per catchment).

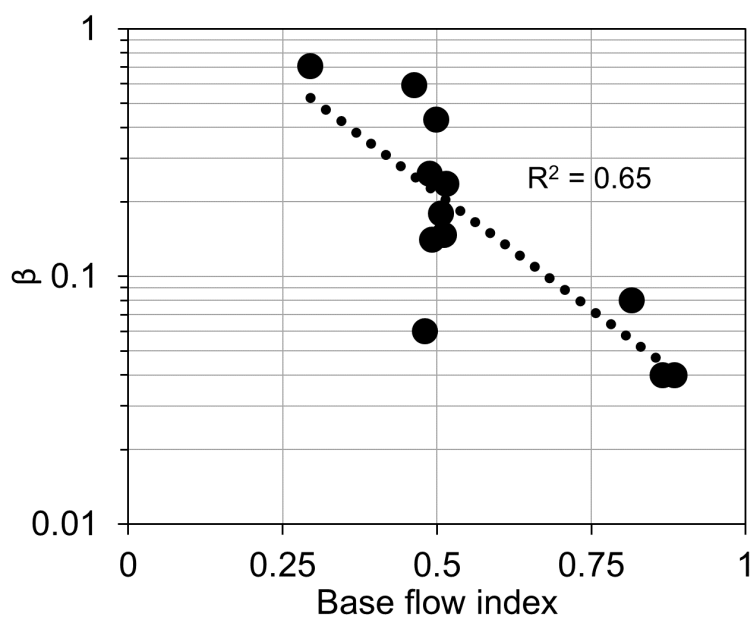


Figure 7. Base flow index (Lyne and Hollick, 1979) versus β . Trendline shows an exponential function.